

Preparation of samarium doped- PMMA composite by casting method to evaluate the optical properties and potential applications

HANAA SHUKER MAHMOOD¹, NADIR FADHIL HABUBI^{2,*}

¹University of Baghdad College of Pure Science, Ibn Alhitham, Baghdad- Iraq

²Department of Radiation and Sonar Technologies, Alnuhba University College, Baghdad, Iraq

Samarium ions (Sm^{+3}), a rare-earth element, have a significant optical emission within the visible spectrum. PMMA samples, mixed with different ratios of $\text{SmCl}_3 \cdot 6\text{H}_2\text{O}$, were prepared via the casting method. The composite was tested using UV-visible, photoluminescence and thermogravimetric analysis (TGA). The FTIR spectrometry of PMMA samples showed some changes, including variation in band intensity, location, and width. Mixed with samarium decreases the intensity of the C-O and CH_2 stretching bands and band position. A new band appeared corresponding to ionic bonds between samarium cations with negative branches in the polymer. These variations indicate complex links between the Sm^{+3} ion and oxygen in the ether group. The optical absorption increased within the visible spectrum while the emission increased. The TGA analysis showed more thermal stability for samples mixed with Sm, where the degradation point shifted to higher energy and with less mass loss in the decomposition region. A triplet band were performed in the emission curve for PMMA reinforced with Sm^{+3} . The outcomes show the possibility of using samarium-enhanced PMMA in optical applications.

(Received August 31, 2022; accepted February 14, 2023)

Keywords: PMMA, Samarium, Optical properties, Thermal stability, FTIR

1. Introduction

Polymethyl methacrylate (PMMA) is a vital polymer for manufacturing polymeric optical fibres in optical communications [1]. It has been used within optical fibres in hydrogen sensing [2], and photoluminescence-based gas sensing [3]. PMMA has used fibre grating-based sensors for moisture sensing [4]. Also, it is used in lithium-ion batteries [5], biomedical applications [6] and denture bases [7]. Doping PMMA with nanoparticles helps change its characteristics, such as optical, structural properties, and stability [8,9]. The polymer's properties can be improved by mixing them with one of the rare-earth elements [10,11]. Combining PMMA with these ions leads to a significant change in numerous features such as optical properties, including absorption [12] and emission spectra for specific wavelengths [13] and quantum effect [14]. The main reason for these changes caused by rare-earth ions is their characteristics of electronic transitions [15]. In addition, the doping level of nanoparticles in a polymer is the limiting factor for improving the quality of the polymeric samples [16].

Hamdalla *et al.* Prepared PMMA films mixed with different rare-earth ions by casting method. They displayed the dependence of optical bandgap and other optical parameters on the characteristic electronic transitions of the ion. They indicate the improvement of PMMA optical fibre with these ions [17]. Nafee *et al.* prepared Er-doped PMMA composite by casting method, the study shows decreasing the energy gap by 6% and a significant enhancement in optical parameters, which designated Er-doped PMMA for use in nonlinear optical

applications[10]. Khurshed *et al.* studied the optical properties of $\text{Sr}_3\text{B}_2\text{O}_6:\text{Dy}^{3+}/\text{PMMA}$ polymer nanocomposites. The luminescent nanocomposite layer presented the characteristic emission and thermal stability increase rather than the un-doped sample [18].

Recent innovations based on PMMA include anti-algae coatings and non-yellowing sheets that give significant protection against UV offered for building applications and waterproofing coating. PMMA films and sheets are often utilized in the building industry because they shield facades from UV radiation, weather protection, and thermal insulating properties [19].

In this study, the fabrication of PMMA mixed with various ratios of Sm^{+3} ions by casting method was done. The study of the doping effect with Sm^{+3} ions on the structural characterization, optical properties and stability to know the appropriateness percentages of this element within the PMMA to improve its properties to make it more applicable in optical applications.

2. Experimental

2.1. Material

PMMA of 120,000 g/mole average molecular weight from Sigma–Aldrich (Germany) and Samarium(III) chloride hexahydrate ($\text{SmCl}_3 \cdot 6\text{H}_2\text{O}$) of 99.9% purity and molecular weight: 364.81 g/mole from Sigma–Aldrich (Germany) are the started materials for this study without any further purification.

2.2. Sample preparation and characterization

PMMA was dissolved in acetone with 1% concentration at 30 °C with continuous stirring. $\text{SmCl}_3 \cdot 6\text{H}_2\text{O}$ at weight ratios of PMMA (1, 2, 3, and 4) wt.% was dissolved in absolute ethanol and then mixed with the PMMA solution using an ultrasonic probe for 10 min to obtain a homogeneous mixture. The mixture was aged for 24 h before being cast into moulds and left to dry for six days to evaporate all solvents completely.

The film of the polymeric sample is about 0.1 mm in thickness. The structural properties for the chemical bands were tested by FTIR technique using (Thermo Scientific Nicolet N10 FTIR Spectrometer) over of 400-4000 cm^{-1} range, and the optical properties were studied, which included UV-visible absorption spectroscopy (SP-8001 spectrophotometer), and emission spectroscopy using (Fluorescence Spectrophotometer F-2700). Finally, thermal properties using TGA analysis (STA PT-1000 device) were done.

3. Results and discussions

Fig. 1 shows the FTIR transmittance spectrum for the prepared PMMA sample. Characteristic bands for PMMA molecular structure have appeared in the pattern. The double band appeared at 3448.06 and 3001.25 cm^{-1} matched with the stretching vibrations of C–H bond for the CH_3 branch [20]. The peak at 1735.29 cm^{-1} is consistent with the C=O vibration in the ester group. The bands at 1470 and 1400 cm^{-1} coordinate with the asymmetric bending vibration of C– CH_2 and C– CH_3 , respectively [21]. The doublet band at (1250, 1266) cm^{-1} consistently stretches the C–O bond in ester groups. The vibration at 1190 cm^{-1} matches the –O– CH_3 stretching within the chain of the PMMA [22]. The band at 730 cm^{-1} corresponds to the asymmetric vibration of CH_2 group [23].

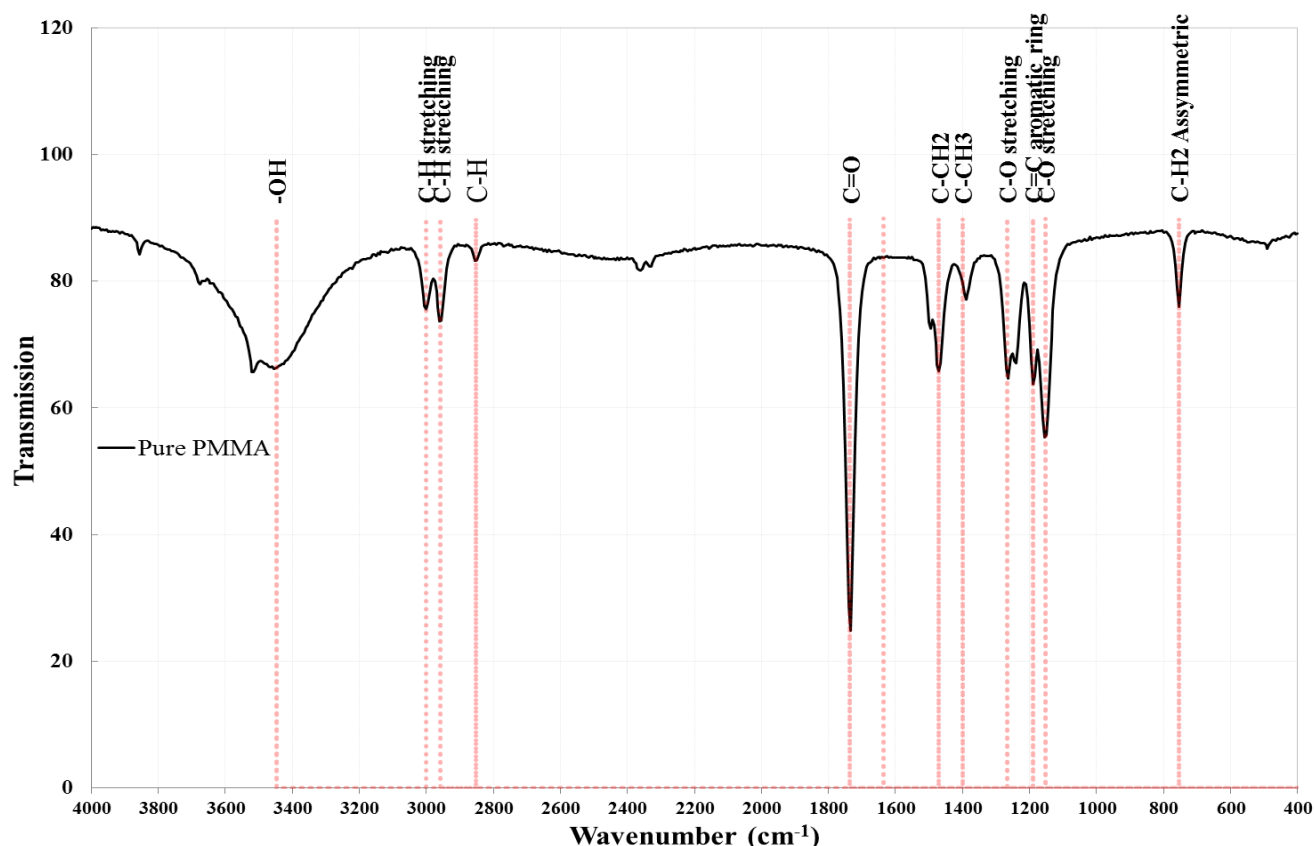


Fig. 1. The FTIR test for the PMMA sample (color online)

Fig. 2 compares the FTIR patterns for pure polymer samples with the doped samples by different proportions with samarium. Some changes seemed in the reinforced samples, such as band intensity, location, and width variations. In addition, a new band at 1635 cm^{-1} corresponds to the bending modes of Sm–OH [24]. There was a variation in the band location of the C=O vibration from 1735 to 1728 cm^{-1} [25]. In addition, this band be more broadening with increasing the samarium ratio to

4%, indicating the interaction of the samarium with the C=O groups of esters, forming a complex structure [17]. The ions can be bound by coordination bonds and covalent bonds with carbonyl group and the O- ether groups of the next layer of polyanion molecules, where the added ions act as binding components. A shift in the C–H bands in CH_3 from 3001–2957 cm^{-1} to 3025–2975 cm^{-1} was also noticed, indicating a reduction of the hydrogen bonds [10]. There are also shifts in the bending bands of C– CH_2 from

1470 to 1460 cm^{-1} for PMMA with increasing the samarium ions ratio due to the presence of some complex formation via the coordination links between the metal and the oxygen in the ether group. The bond of C-O in the

ester groups shifted to a lower frequency from 1240 to 1230 cm^{-1} due to the attractive force between the oxygen and the added ions [26].

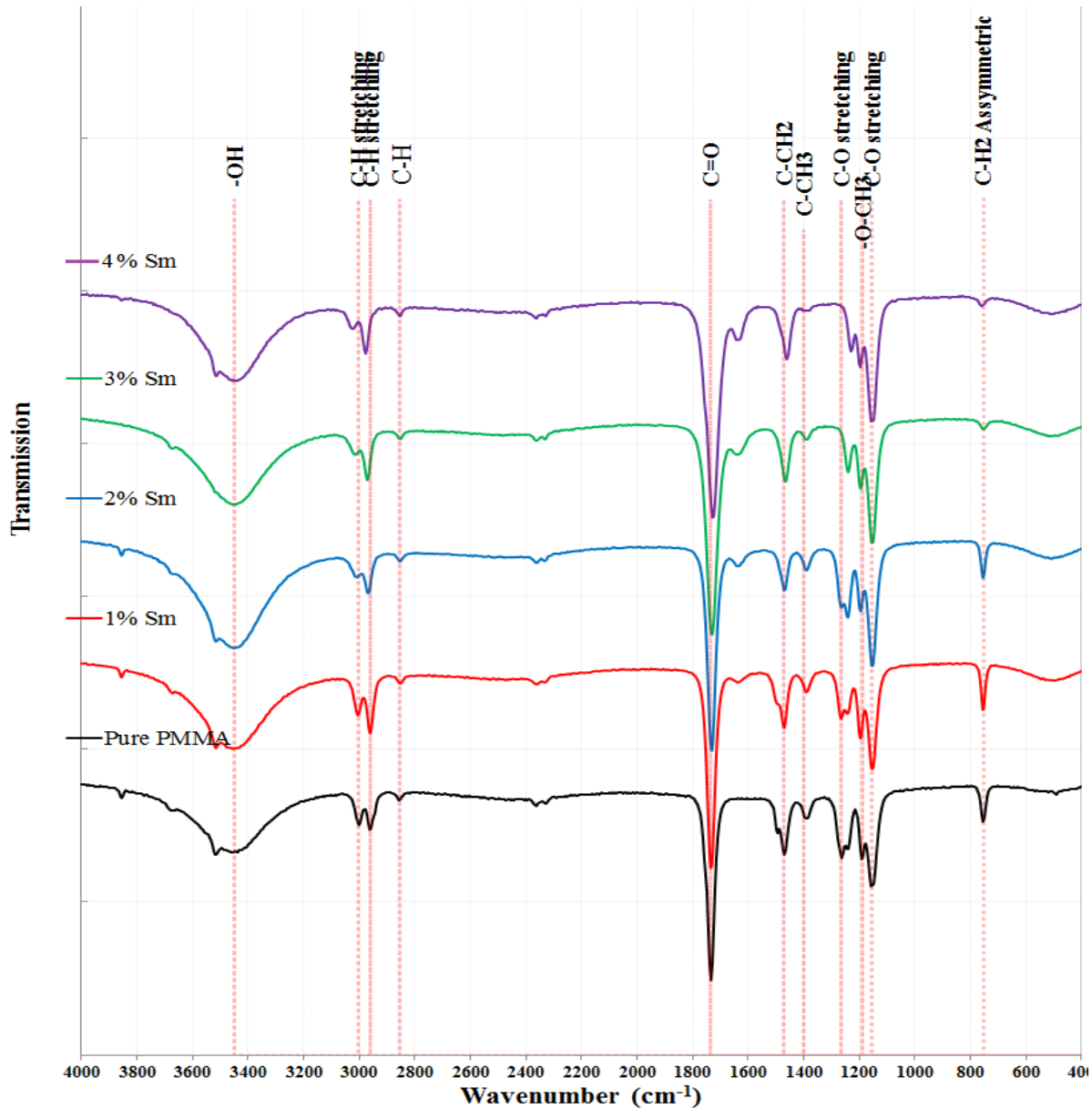


Fig. 2. The FTIR curves for pure and Sm-doped PMMA samples at different ratios (color online)

Thermal stability was tested using thermogravimetric analysis (TGA) performed at atmospheric pressure in the evidence of nitrogen for each pure sample and the PMMA: Sm composite at 4% percentage. Fig. 3 displays the TGA assay result. A tremendous weight loss was seen between temperatures of 300°C and 400°C. The first level of weight loss of 5.9% around 100 °C is moisture loss. The second level of weight loss region starts at the onset point at 300°C reaching about 81.8 % at 400°C, which can be

recognized as the decomposition region of the polymer. The PMMA: Sm composite starts decomposing at the onset point of 320°C and suffers a lesser loss of about 74.3% at the decomposition region.

Indicates the significant effect of doping with Sm ions on thermal stability due to its interaction with the polymer chain. Better thermal stability can be founded on PMMA matrices which provide a more stable against the environmental effect.

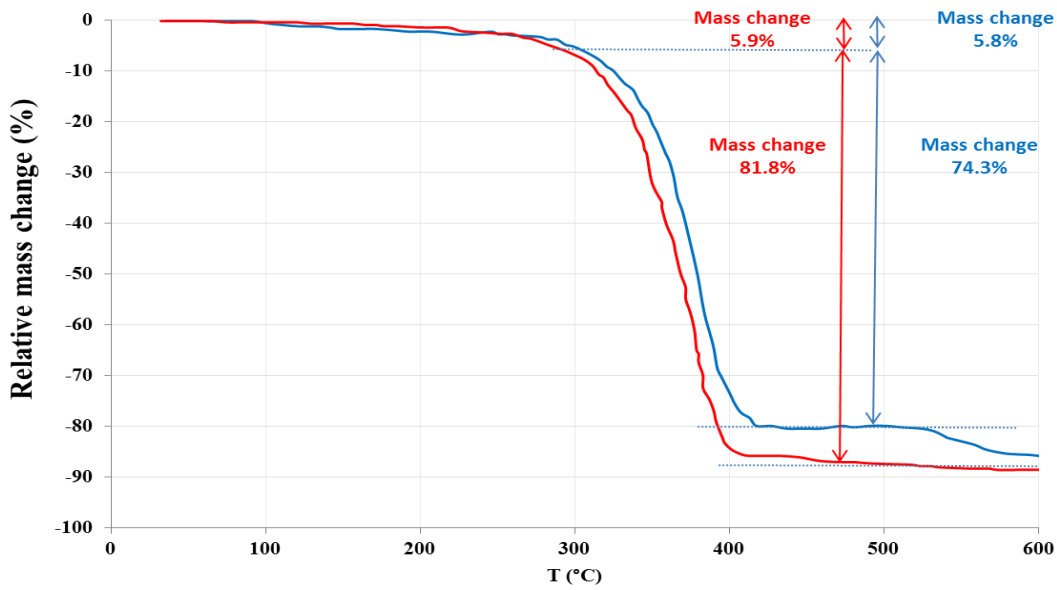


Fig. 3. The TGA for pure PMMA and doped with Sm at 4% weight percentage (color online)

Fig. 4 illustrates the UV-visible absorbance curves for the PMMA polymer and doped samples with samarium ions at different ratios. The absorbance increased with the concentrations of samarium ions, especially in the UV

range. So, enhancement of UV absorption makes their coating provide more protection against UV radiation. This result agrees with previous studies [27,28].

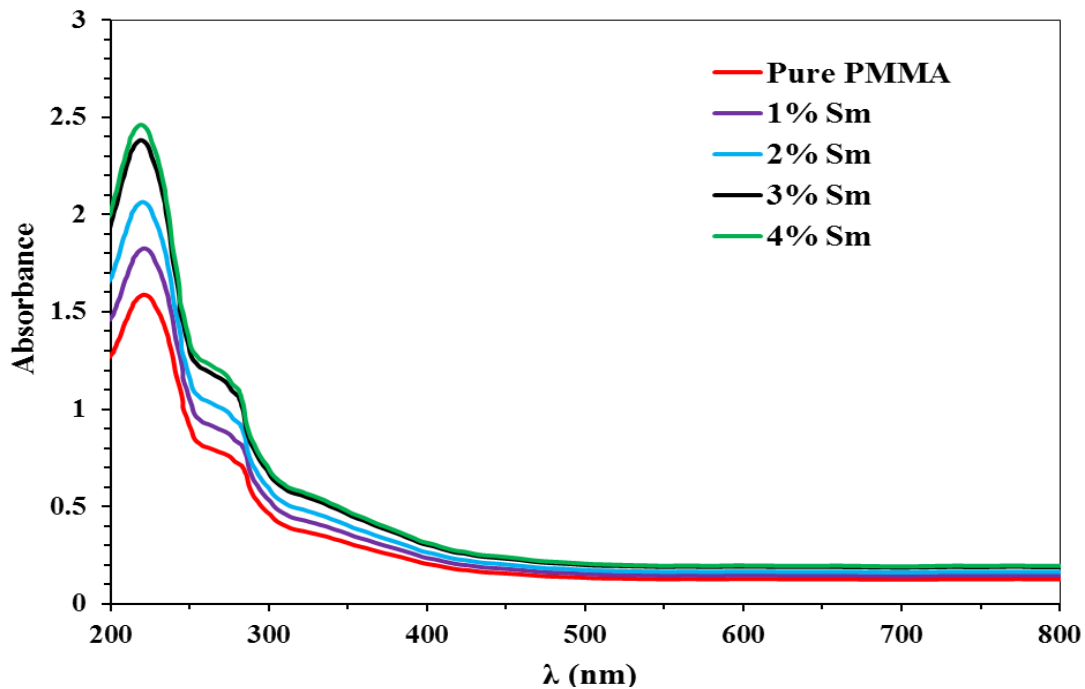


Fig. 4. The UV-visible absorption for pure and Sm-doped PMMA samples at different weight ratios (color online)

The Sm-doped PMMA composite's photoluminescence was examined and compared with the pure PMMA sample, under excitation of 350 nm, as shown in Fig. 5. The spectra show broad emission bands centered at 500 nm and 470 nm for PMMA and Sm/PMMA composite, respectively, corresponding to the $\pi \rightarrow \pi^*$ transition [23].

The notable change between PL intensity of Sm/PMMA and PMMA is value examining. The PL spectrum of the Sm-doped PMMA composite shows three peaks located at 560, 595, and 640 nm for the characteristic transitions $^4G_{5/2} \rightarrow ^6H_{5/2}$, $^4G_{5/2} \rightarrow ^6H_{7/2}$, and $^4G_{5/2} \rightarrow ^6H_{9/2}$ of samarium, respectively [29]. The results can be a promising candidate for optical applications, such

as luminescent solar concentrator applications, to enhance their conversion efficiency and LED application [30,31].

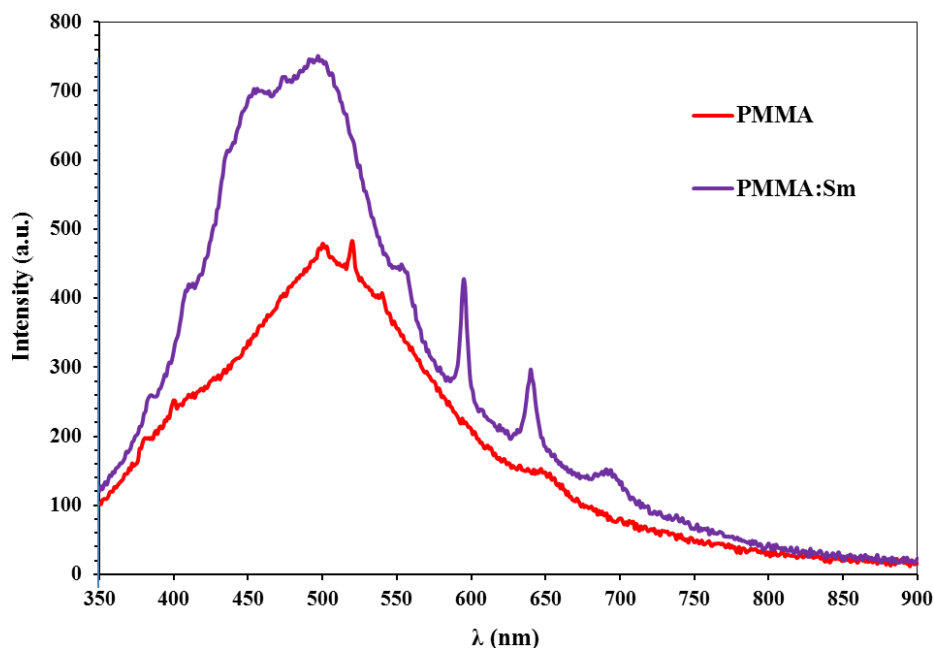


Fig. 5. The PL for pure and doped PMMA samples with Sm at 4% weight ratios (color online)

4. Conclusions

The prepared PMMA samples doped with Sm ions at different weight percentages by the casting method show the following variations. The FTIR spectrometry examination showed that mixed in samarium at different ratios leads to the emergence of a new C = O group, while the C-O band decreases in intensity. The results show an increased absorption, especially in the UV range, with the Sm ratio. The TGA analysis shows more thermal stability for samples mixed with Sm, even by a few degrees Celsius after doping. Under ultraviolet excitation, the PMMA presents an emission band of broad features around 500 nm consistent with the $\pi \rightarrow \pi^*$ transition of PMMA. At the same time, the mixed sample shows additional peaks agreeing with characteristic bands of Sm, which transfer energy efficiently from the polymer to Sm ions. The results indicate the possibility of using samarium-enhanced PMMA in optical applications, such as UV protection or luminescent solar concentrator applications.

Acknowledgements

Authors would thank the university of Baghdad and Alnuhba University College for their support.

References

- [1] J. Gamboa, J. Vonckx, M. Fouda, S. M. Shahriar, in: *Front. Opt. / Laser Sci.*, OSA, Washington, D.C., FW7A.1 (2020).
- [2] H. Bai, G. Shi, *Sensors* **7**, 267 (2007).
- [3] O. Marantos, V. Binas, M. Moschogiannaki, E. Gagaoudakis, G. Kiriakidis, A. Klini, *Mater. Sci. Semicond. Process* **133**, 105942 (2021).
- [4] L. S. M. Alwis, T. Sun, K. T. V. Grattan, *Procedia Eng.* **168**, 1317 (2016).
- [5] T. Zhang, H. Qu, K. Sun, *Mater. Lett.* **245**, 10 (2019).
- [6] Y. H. Li, X. Y. Shang, Y. J. Li, *Mater. Lett.* **270**, 127744 (2020).
- [7] D. H. Mohammed, M. S. Tukmachi, I. N. Safi, *Mater. Today Proc.* **42**, 2482 (2021).
- [8] B. M. Jaffar, H. C. Swart, H. A. A. Seed Ahmed, A. Yousif, R. E. Kroon, *J. Phys. Chem. Solids* **131**, 156 (2019).
- [9] M. A. Forte, R. M. Silva, C. J. Tavares, R. F. E Silva, *Polymers (Basel)* **13**, 1346 (2021).
- [10] S. S. Nafee, T. A. Hamdalla, A. A. A. Darwish, *Opt. Laser Technol.* **129**, 106282 (2020).
- [11] C. Liu, R. Deng, Y. Gong, C. Zou, Y. Liu, X. Zhou, B. Li, *Int. J. Photoenergy* **2014**, 1 (2014).
- [12] Y. Khairy, M.I. Mohammed, H.I. Elsaedy, I. S. Yahia, *Optik* **212**, 164687 (2020).
- [13] R. Piramidowicz, A. Jusza, L. Lipińska, M. Baran, P. Polis, A. Olszyna, *J. Lumin.* **226**, 117458 (2020).
- [14] F. Hu, X. Liu, R. Chen, Y. Liu, Y. Mai, R. Maalej, Y. Yang, *J. Rare Earths* **35**, 964 (2017).
- [15] Y. H. Elbashar, D. A. Rayan, *Int. J. Appl. Chem.* **12**, 59 (2016).
- [16] Z. Chen, Y. Zhu, X. Guo, M. Li, M. Ge, *J. Lumin.* **199**, 1 (2018).
- [17] T. A. Hamdalla, T. A. Hanafy, S. M. Seleim, *Phase Transitions* **92**, 603 (2019).
- [18] S. Khursheed, V. Kumar, V. K. Singh, J. Sharma, H. C. Swart, *Phys. B Condens. Matter* **535**,

- 184 (2018).
- [19] C. Queant, P. Blanchet, V. Landry, D. Schorr, *J. Polym. Eng.* **39**, 94 (2018).
- [20] R. Huszank, E. Szilágyi, Z. Szoboszlai, Z. Szikszai, *Nucl. Instruments Methods Phys. Res. B* **450**, 364 (2019).
- [21] L. Huang, H. Jiang, W. Gao, *Journal of the Loss Prevention in the Process Industries* **71**, 104515 (2021).
- [22] A. León, P. Reuquen, C. Garín, R. Segura, P. Vargas, P. Zapata, P. Orihuela, *Appl. Sci.* **7**, 49 (2017).
- [23] R. J. Sengwa, S. Choudhary, P. Dhatarwal, *Adv. Compos. Hybrid Mater.* **2**, 162 (2019).
- [24] T. Seki, K.-Y. Chiang, C.-C. Yu, X. Yu, M. Okuno, J. Hunger, Y. Nagata, M. Bonn, *J. Phys. Chem. Lett.* **11**, 8459 (2020).
- [25] H. Yasuda, *J. Polym. Sci. Part A Polym. Chem.* **39** 1955–1959 (2001).
- [26] S. Ramesh, K.H. Leen, K. Kumutha, A. K. Arof, *Spectrochim. Acta - Part A Mol. Biomol. Spectrosc.* **66**, 1237 (2007).
- [27] W. Fan, J. Feng, S. Song, Y. Lei, L. Zhou, G. Zheng, S. Dang, S. Wang, H. Zhang, *Nanoscale* **2**, 2096 (2010).
- [28] M. Alsawafta, S. Badilescu, A. Paneri, V. Van Truong, M. Packirisamy, *Polymers* **3**, 1833 (2011).
- [29] M. Luo, B. Chen, X. Li, J. Zhang, S. Xu, X. Zhang, Y. Cao, J. Sun, Y. Zhang, X. Wang, Y. Zhang, D. Gao, L. Wang, *Phys. Chem. Chem. Phys.* **22**, 25177 (2020).
- [30] W. Zhou, M.-C. Wang, X. Zhao, *Sol. Energy* **115**, 569 (2015).
- [31] S. Khursheed, P. Biswas, V. K. Singh, V. Kumar, H. C. Swart, J. Sharma, *Vacuum* **159**, 414 (2019).

* Corresponding author: n.fadhil@alnukhba.edu.iq